THE JOURNAL OF BIOLOGICAL CHEMISTRY
Vol. 274, No. 27, Issue of July 2, pp. 19181–19187, 1999

Printed in U.S.A.

Lys[13] Plays a Crucial Role in the Functional Adaptation of the Thermophilic Triose-phosphate Isomerase from *Bacillus stearothermophilus* to High Temperatures*

(Received for publication, February 5, 1999, and in revised form, March 11, 1999)

Marco Alvarez‡§, Johan Wouters¶, Dominique Maes‖, Véronique Mainfroid‡, Françoise Rentier-Delrue‡, Lode Wyns‖, Eric Depiereux¶, and Joseph A. Martial‡ ‡‡**

From the ‡Laboratoire de Biologie Moléculaire et de Génie Génétique, Université de Liège, B6, Sart Tilman, B4000 Liège, Belgium, ¶Laboratoire de Biologie Moléculaire Structurale, Facultés Universitaires Notre-Dame de la Paix, B5000 Namur, Belgium, and ‖Ultrastructure Unit, Vlaams Interuniversitair Instituut voor Biotechnologie, Vrije Universiteit Brussel, B1640 Sint-Genesius-Rode, Belgium

The thermophilic triose-phosphate isomerases (TIMs) of *Bacillus stearothermophilus* (bTIM) and *Thermotoga maritima* (tTIM) have been found to possess a His[12]-Lys[13] pair instead of the Asn[12]-Gly[13] pair normally present in mesophilic TIMs. His[12] in bTIM was proposed to prevent deamidation at high temperature, while the precise role of Lys[13] is unknown. To investigate the role of the His[12] and Lys[13] pair in the enzyme's thermoadaptation, we reintroduced the "mesophilic residues" Asn and Gly into both thermophilic TIMs. Neither double mutant displayed diminished structural stability, but the bTIM double mutant showed drastically reduced catalytic activity. No similar behavior was observed with the tTIM double mutant, suggesting that the presence of the His[12] and Lys[13] cannot be systematically correlated to thermoadaptation in TIMs. We determined the crystal structure of the bTIM double mutant complexed with 2-phosphoglycolate to 2.4-Å resolution. A molecular dynamics simulation showed that upon substitution of Lys[13] to Gly an increase of the flexibility of loop 1 is observed, causing an incorrect orientation of the catalytic Lys[10]. This suggests that Lys[13] in bTIM plays a crucial role in the functional adaptation of this enzyme to high temperature. Analysis of bTIM single mutants supports this assumption.

Understanding the molecular adaptation of proteins to extreme temperatures remains a major challenge for protein scientists. Over the last 2 decades, several studies have attempted to establish a general rule leading to thermostability, but no overall consensus explanation could be formulated (1). For example, although the composition of thermophilic proteins shows that certain amino acids are preferred to ones present in mesophilic homologues, no general trends emerge. Studies have demonstrated the need to place the analysis of primary structure in a three-dimensional structural context (2); structural determinants such as ionic networks (3, 4), hydrophobic packing (5, 6), and cooperative associations (5, 7) seem to better reflect the general features associated with thermal adaptation. All of them, individually or in combination, enable thermophilic proteins to adapt to extreme temperatures.

Thermotoga maritima is a hyperthermophilic eubacterium of the order Thermotogales, the oldest branch within the bacterial domain. Its optimal growth temperature is 80 °C (8). *Bacillus stearothermophilus* is a moderately thermophilic endospore-forming Gram-positive rod growing optimally at about 65 °C (9). Several glycolytic pathway enzymes from these strains have been produced by recombinant DNA technology, and all of them display optimal catalytic activity at temperatures above the optimal growth temperature of the source organism (1). Triose-phosphate isomerase (TIM)[1] is one of them.

TIM is a homodimer catalyzing the interconversion of dihydroxyacetone phosphate and D-glyceraldehyde 3-phosphate in the glycolytic pathway (10). It is the prototype of a family comprising many different members sharing a common folding motif called the α/β barrel. This fold consists of eight parallel β-strands forming a barrel, surrounded by eight α-helices (11). The active site of TIM lies at the carboxyl-terminal end of the β-barrel, and the catalytic residues belong to loops connecting the β-strands to the following α-helices (Lys[10], His[94], and Glu[166]; *B. stearothermophilus* TIM numbering). At present, the three-dimensional structures of 11 TIMs are known: those of chicken (12), yeast (13), *Trypanosoma brucei* (14), *Escherichia coli* (15), human (16), *B. stearothermophilus* (17), *Plasmodium falciparum* (18), *Vibrio marinus* (19), *Trypanosoma cruzei* (20), *Leishmania mexicana* (21), and *T. maritima*.[2]

B. stearothermophilus TIM (bTIM) is reported to display moderately thermophilic enzymatic properties (22). Resolution of its crystallographic structure has made it possible to propose

* This work was supported by Actions de Recherche Concertées Convention Grant 95/00–193, Services Fédéraux des Affaires Scientifiques, Techniques et Culturelles (SSTC) Grant PAI P4–30, SSTC Convention PRODEX ESA contract 1298/98/NL/VJ, and the Fonds National de la Recherche Scientifique Convention Grant FRFC 2.4545.96. Funding by the Belgian National Science Foundation (FWO) and Vlaams Interuniversitair Institout voor Biotechnologie supported the crystallographic work. The x-ray data were collected at station 9.5 of the Synchrotron Radiation Source in Daresbury, United Kingdom. The costs of publication of this article were defrayed in part by the payment of page charges. This article must therefore be hereby marked "*advertisement*" in accordance with 18 U.S.C. Section 1734 solely to indicate this fact.

The atomic coordinates and structure factors of H12N/K13G bTIM (code 2BTM) have been deposited in the Protein Data Bank, Brookhaven National Laboratory, Upton, NY.

§ Recipient of a fellowship from the Patrimoine de l'Université de Liège.

** Research associate of the FWO.

‡‡ To whom correspondence may be addressed: Laboratoire de Biologie Moléculaire et de Génie Génétique, Université de Liège, B6, Sart Tilman, B4000 Liège, Belgium. Tel.: 32-4-3663371; Fax: 32-4-3662968; E-mail: jmartial@ulg.ac.be.

[1] The abbreviations used are: TIM, triose-phosphate isomerase; tTIM and bTIM, TIM of *T. maritima* and *B. stearothermophilus*, respectively; PCR, polymerase chain reaction; MES, 4-morpholineethanesulfonic acid; r.m.s., root mean square.

[2] D. Maes, J. P. Zeelen, N. Thanki, N. Beaucamp, M. Alvarez, M. H. Dao-Thi, J. Backmann, J. A. Martial, L. Wyns, R. Jaenicke, and R. K. Wierenga, manuscript in preparation.

certain features as responsible for its increased thermostability, such as higher content of proline residues at the N1 position in helices, smallest number and volume of cavities, and more buried hydrophobic surfaces upon dimerization than *E. coli* TIM (17).

T. maritima TIM (tTIM), described by Schurig *et al.* (23), is an extremely thermophilic protein resistant to temperatures above 90 °C. Surprisingly, it is produced as a fusion protein jointly with phosphoglycerate kinase, another glycolytic enzyme. Recently, it has been proposed that the tetrameric quaternary structure adopted by the polyprotein permits conservation of the dimeric form necessary for TIM activity and increases slightly the thermal stability of tTIM (24).

Although many TIM sequences have been reported, few of these proteins have been fully characterized in terms of thermal stability. Alignment of these sequences reveals a particular pair substitution in one of the conserved regions of "thermophilic TIMs" (bTIM and tTIM), an N12H/G13K replacement. Residues 12 and 13 belong to a region of variable length named loop 1, joining strand β1 to helix α1 and located at the TIM dimer interface. The presence of the His[12]-Lys[13] pair is also present in the TIM of a *Synechocystis* sp. strain, a mesophilic cyanobacterium (25). His[12] has been found in the TIMs of *Pseudomonas syringae*[3] and *Borrelia burgdorferi* (27), and Lys[13] has been found in *Bacillus subtilis* TIM (28), but there is no available information on the enzymatic properties and stability of these TIMs.

The high conservation of Asn[12] in most TIMs can be explained by the ability of the Asn side chain amide nitrogen to interact with residues Trp[9] and Met[11] of the same loop, thereby stabilizing the catalytic Lys[10] of the active site (17). At high temperature, an Asn residue at the edge of the protein's dimeric interface (partially solvent-exposed) is susceptible to deamidation leading to irreversible heat inactivation of the enzyme (29). In solution, deamidation occurs through intramolecular nucleophilic attack by the backbone amide nitrogen on the γ-carbonyl carbon of the Asn side chain, resulting in conversion of Asn residues to aspartate or isoaspartate and release of ammonia (30). The rate of deamidation in proteins depends on the pH, ionic strength, temperature, sequence, and structure (30–32). Replacement of Asn residues is used in protein engineering to thermostabilize proteins: in *Aspergillus awamori* glucoamylase, for instance, it was possible to increase its thermostability severalfold (33). Furthermore, Asn residues followed by Gly appear considerably more sensitive to deamidation (34–36) because Gly has more freedom in its main chain torsion angles. This effect was measured by altering Asn-Gly sequences in lysozyme; substitution of Ala for Gly in these sequences protected the enzyme against irreversible heat inactivation (37). In human and yeast TIMs, two deamidation-sensitive regions have been identified, one in loop 1 and one in loop 3 (29, 38, 39).

Considering all of these factors, it has been proposed that the N12H and G13K replacements in bTIM could be deamidation-preventing molecular adaptations of the enzyme (17). Since the same replacements are also observed in tTIM, it was interesting to see whether this might be part of a general thermostabilization process in TIM. In the present work we have produced double mutants by reintroducing Asn and Gly residues at positions 12 and 13, respectively, in thermophilic bTIM and tTIM. We have measured the activity and structural stability of the mutant enzymes and resolved the three-dimensional structure of the bTIM double mutant. We discuss the individual role of each residue in bTIM and tTIM stability.

MATERIALS AND METHODS

Bacterial Strains, Plasmids, and DNA—The *E. coli* strain HB101 (*SupE44 hsd S20 rB-mB recA13ara-14 pro A2 lacY1 gal K2rpsL20xyl-5mtl-1*) was used for DNA cloning. The *E. coli* strain BL21(DE3) (*hsd S gal cIts 857 ind1 Sam7 nin5 lacUV-T7*, gene 1) was used for protein production. The tTIM gene was overexpressed in the pARAE vector (40), a derivative of pAR3040 (41). *T. maritima* genomic DNA was kindly provided by N. Glansdorff (Research Institute of the CERIA-COOVI, Brussels, Belgium).

Cloning of the tTIM Gene—A polymerase chain reaction (PCR) was performed on *T. maritima* genomic DNA, using degenerated primers corresponding to conserved regions of TIM (5′-GGNAAYTGGAA-3′ and 5′-NGTNCCNATNGCCCA-3′) (22). A 500-base pair fragment of the TIM gene was obtained. The entire TIM gene sequence was obtained by inverse PCR (42). Briefly, *T. maritima* genomic DNA was cut with *Eco*RI, and fragments were recircularized by ligation. The ligated fragments were used as templates for PCR, using primers complementary to sequences located near the ends of the 500-base pair TIM fragment. The amplification reaction resulted in a head-to-tail arrangement of the sequences originally flanking the target region. This product was cloned and sequenced. To obtain the complete TIM gene, we performed another PCR starting with *T. maritima* chromosomal DNA, using primers corresponding to regions flanking the TIM gene. The tTIM gene PCR product was cloned into the pCRII plasmid (TA cloning system, Invitrogen Corp.). Several clones were sequenced in both directions in order to find clones without errors potentially introduced by *Taq* polymerase. The correct clone was called gTm10.

Construction of the tTIM and bTIM Expression Vectors—The tTIM gene was isolated from the gTm10 vector by PCR, using the following primers: 5′-GCTCTAGAGGCATATGATAACTCGTAAACTG-3′, containing *Xba*I and *Nde*I restriction sites (underlined), followed by the first five codons encoding the first five amino acid residues of tTIM, and 5′-TGTTTCTCCTTCGTTTCTCT-3′, complementary to the tTIM nucleotide sequence located 466–485 base pairs downstream from the ATG. The PCR product was cut with *Xba*I and *Ava*I, purified and ligated to the digested gTm10 plasmid, and finally sequenced. This new plasmid was then cut with *Nde*I and *Bam*HI to isolate the entire TIM gene, which was subsequently ligated into the *Nde*I and *Bam*HI sites of the expression vector pARAE. The plasmid obtained was called pT_7-Ther. The expression vector used for bTIM production (named pT_7im-Bac) was from Rentier-Delrue *et al.* (22).

Site-directed Mutagenesis—Site-directed mutagenesis was performed on the pT_7-Ther and pT_7im-Bac vectors using the Chameleon Kit (Stratagene). Double mutants of tTIM and bTIM, containing the H12N and K13G replacements, were constructed using the following oligonucleotides: 5′-CCGAGATCGTGCCGTTCATCTTCCAGTTCC-3′ (for tTIM) and 5′-CCGCTAATGTGCCGTTCATTTTCCAGTTGCC-3′ (for bTIM) (mutated codons are underlined). The individual mutations produced in the bTIM gene were incorporated using the following oligonucleotides: 5′-CCGCTAATGTTTTGTTCATTTTCCAGTTGCCTGC-3′ (for the H12N replacement) and 5′-CCGCTAATGTGCCATGCATTTTCCAGTTGCCTGC-3′ (for the K13G replacement). The oligonucleotides were purchased from Eurogentec, S. A. (Seraing, Belgium).

Production and Purification of the Wild-type and Mutant TIMs—The proteins were overproduced using the T7 system (43). *E. coli* BL21(DE3) cells carrying the expression vectors were grown for 16 h at 37 °C in L broth medium containing 100 mg/l ampicillin. Induction with isopropyl-β-D-thiogalactopyranoside was unnecessary for protein production. Under these conditions, the proteins were produced in a soluble form. The cultures were centrifuged for 15 min at 4500 × *g*, and the pellets were resuspended in 20 mM triethanolamine HCl buffer, pH 7.6. The cells were disrupted in a high pressure cell (Inceltech, S. A.), and the cell debris was eliminated by centrifugation (45 min, 10,000 × *g*).

The supernatants were fractionated by ammonium sulfate precipitation, and the TIM-containing fractions were dialyzed overnight at room temperature against 20 mM triethanolamine HCl buffer, pH 7.6. The dialyzed samples were then applied to a Mono Q ion exchange column (HR 10/10, Amersham Pharmacia Biotech) pre-equilibrated in the same buffer. Proteins were eluted from the column with a 0–500 mM NaCl gradient, and the TIM-containing fractions were pooled. Samples containing wild-type TIM were incubated for 10 min at 70 °C and centrifuged for 30 min at 10,000 × *g*. Sample purity was monitored by SDS-polyacrylamide gel electrophoresis (15% polyacrylamide). Protein concentrations were determined by the Bio-Rad protein assay with

[3] J. J. Rich and D. K. Willis, nucleotide sequence of *Pseudomonas syringae* TIM, ID TPIS-PSESY, Swiss-Prot Data Bank code (AC) P95576.

bovine serum albumin as the standard.

Enzymatic and Stability Assays—TIM activity assays were performed as described by Misset and Opperdoes (44). The assay mixture contained 0.24 mM NADH (Roche Molecular Biochemicals), 20 μg/ml glycerol-3-phosphate dehydrogenase (Roche Molecular Biochemicals), 9.75 mM D-glyceraldehyde 3-phosphate (Sigma), and 100 mM triethanolamine HCl buffer (pH 7.6). The assay was started by the addition of the following enzyme: 0.8 ng of tTIM, 8.9 ng of bTIM, 4.2 ng of the H12N/K13G bTIM double mutant, 32 ng of the H12N/K13G tTIM double mutant, 11 ng of the H12N bTIM mutant, or 7.4 ng of the K13G bTIM mutant.

The thermal stability of each protein was tested by incubating the reaction mixtures at temperatures ranging from 25 to 95 °C in a Triothermoblock TB-1 (Biometra BAU). Residual activity after incubation was measured at 25 °C. The inactivation rate constant at each temperature (k_{inact}, expressed in s^{-1}) is defined as the slope of the $\ln(A_t/A_o)$ *versus* the incubation time (22).

Calorimetric Studies—Differential scanning calorimetry was performed in a Micro Calorimetry System differential scanning calorimetric unit (MicroCal, Inc.). The protein concentration was adjusted to 1.5 mg/ml for all proteins. Scanning was from 25 to 110 °C (tTIM and H12N/K13G tTIM) and from 25 to 90 °C (bTIM and its mutants) at a scan rate of 1 °C/min.

Crystallization and Data Collection—Crystals were grown at 20 °C using the hanging drop vapor diffusion technique under conditions similar to those used to crystallize the wild-type enzyme. The protein solution contained 7 mg/ml protein in 5 mM MES (pH 6.5), 1 mM EDTA, 1 mM sodium azide, 2 mM 2-phosphoglycolate (an inhibitor of the protein). Drops were prepared by mixing 4 μl of protein solution with 3 μl of reservoir solution composed of 25% (w/v) polyethylene glycol 4000, 8% isopropyl alcohol, 100 mM acetate buffer (pH 5.0), 1 mM EDTA, 1 mM sodium azide, and 2 mM dithiothreitol. Needle-shaped crystals were formed. Data were collected to 2.4 Å from one crystal at 20 °C on a Big Mar image plate at station 9.5 of the Daresbury synchrotron source. A wavelength of 1.1 Å was used. The data set was processed with DENZO (45). Scaling, merging, and reduction of the integrated intensities were done with SCALEPACK (45) and TRUNCATE (46). The crystal lattice is primitive orthorhombic with a = 78.13 Å, b = 107.91 Å, and c = 70.98 Å. Because the cell parameters were the same as for native bTIM, the same packing as in the native cell was expected, belonging to space group $P2_12_12$. Hence, no molecular replacement was done. The coordinates of native bTIM (1BTM; Protein Data Bank, Brookhaven National Laboratory, Upton, NY) were immediately used for rigid body refinement. The *R*-factor for data between 9 and 3.0 Å dropped to 26.6% for this solution. Data collection statistics are summarized in Table I.

Refinement and Quality of the Structure—A few rounds of visual inspection and improvement followed by computer refinement took place. On the one hand, the model was optimized with the program O (47) running on an SGI workstation, to improve its fit into a 2Fo-Fc density map. On the other hand, refinement was pursued by combining simulated annealing x-ray refinement and conventional positional and thermal factor refinement, using the X-PLOR (48) package. For refinement, a subset of 5% of the data (the test set) was used for *R*-free calculations. A bulk solvent correction was applied. In one of the first rounds, the sequence was changed to the mutated one in both monomers. Electron density maps indicated a closed conformation for loop 6, which was manually rebuilt into the density map. In addition and as expected, the 2-phosphoglycolate molecule was found in the active site of each subunit. Its coordinates were included in the model. The final refinement stages were carried out with crystallography and NMR system (49). Water molecules were added at sites displaying a peak larger than three S.D. values above the mean in an Fo-Fc map and having a potential hydrogen bonding partner. A total of 121 water molecules were identified. The final *R*-factor is 17.5%, and *R*-free is 22.0% for all data in the resolution range from 30 to 2.40 Å. The quality of the structure was analyzed with the programs PROCHECK (50) and WHAT IF (51). The refinement statistics are summarized in Table I.

Molecular Dynamics Simulation—Energy minimizations (molecular dynamics and molecular mechanics) were performed with the Discover program DM1 (Discover User Guide, Molecular Simulations, San Diego), using the cvff force field. Graphical displays were generated with the InsightII molecular modeling system DM2 (InsightII User Guide, Molecular Simulations, San Diego). Computations were done on a Silicon Graphics Indigo2 workstation running Irix 5.3. The three-dimensional coordinates of bTIM, tTIM, and H12N/K13G bTIM were taken from the corresponding crystallographic structures for bTIM (1BTM; Protein Data Bank, Brookhaven National Laboratory, Upton, NY), tTIM,[2] and the double mutant bTIM (this work). Three-dimensional structures of the single mutants H12N bTIM and K13G bTIM were generated with the Builder interface of the InsightII program, starting with the experimental structure of bTIM. The coordinates of the ligand (2-phosphoglycolate in bTIM and a sulfate ion in tTIM) were retained in the structures, while water molecules were removed. Hydrogens were automatically assigned. A distance-dependent (1.r) dielectric constant was used. For simulations, a subset was defined for each structure, containing all amino acids of the protein within 18 Å of the active site. All coordinates (main chain and lateral chain) were fixed except those of loop 1 (residues 9–20 and 11–22 in bTIM and tTIM, respectively). A combination of molecular mechanic runs (steepest descent + conjugated gradient + Newton-Raphson) was first applied to the structures in order to define equivalent inputs for the molecular dynamics simulations. This was done as the starting structures were obtained at different levels of precision (different resolutions). Molecular dynamics ensued at 300 K for a total of 100 ps (20 runs of 5000 fs), generating 20 geometries for each structure. The geometries were further minimized (annealing to a final derivative cut-off of 0.05 kcal/mol) and analyzed.

TABLE I
Crystallographic data and refinement statistics

Parameters	Values
Crystal data	
Space group	$P2_12_12$
Cell dimensions (Å)	78.132; 107.913; 70.980
Cell dimensions (degrees)	90.0 90.0 90.0
Subunits per asymmetric unit	2
Data collection statistics	
Observed reflections	70,035
Unique reflections	22,732
Overall range (Å)	30.0–2.4
Overall *R*-merge (%)	7.3
Overall completeness (%)	94.3
Last shell range (Å)	2.49–2.40
Last shell *R*-merge (%)	27.8
Last shell completeness (%)	65
Refinement	
Protein atoms	3672
Ligand atoms	18
Solvent atoms	121
Resolution range (Å)	30.0–2.4
R-factor (%)	17.5
R-free (%)	22.0
r.m.s. bond length deviations (Å)	0.006
r.m.s. bond angle deviations (degrees)	1.253
r.m.s. ΔB for bonded main chain atoms (Å^2)	1.392
r.m.s. ΔB for bonded side chain atoms (Å^2)	2.529
Average *B*-factor, all protein atoms (Å^2)	27.9
Average *B*-factor, backbone atoms (Å^2)	27.1
Average *B*-factor, side chain atoms (Å^2)	28.8
Average *B*-factor, ligand atoms (Å^2)	25.7
Average *B*-factor, solvent atoms (Å^2)	29.7
Ramachandran plot[a]	
Most favored regions (%)	92.3
Additionally allowed regions (%)	7.7
Generously allowed regions (%)	0.0
Disallowed regions (%)	0.0

[a] As defined by PROCHECK (50).

RESULTS

Enzymatic Stability—By *in vitro* site-directed mutagenesis we replaced the residues His[12] and Lys[13] of bTIM and tTIM with Asn and Gly, respectively, these two residues being often found in mesophilic TIMs. The two single point mutants H12N bTIM and K13G bTIM were also generated in order to assess the individual role of each residue. The wild-type and mutant TIMs were produced in *E. coli* as soluble recombinant proteins.

The catalytic activities of bTIM, tTIM, H12N/K13G tTIM, H12N/K13G bTIM, H12N bTIM, and K13G bTIM were measured over a range of temperatures close to the optimal growth temperature of the parent bacterial strain (Fig. 1). Under these conditions, wild-type recombinant tTIM proved very stable, having a half-life of 11.5 min at 94 °C. This is in agreement with the half-life reported for tTIM by Beaucamp *et al*. (24). Surprisingly, H12N/K13G tTIM appears slightly more stable,

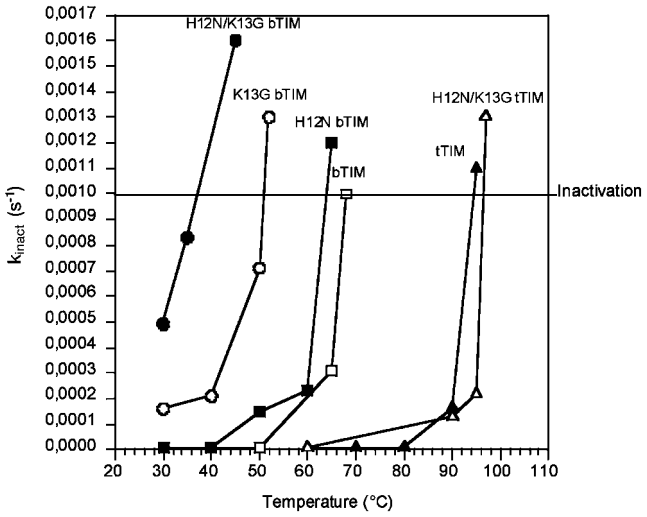

FIG. 1. **Thermal inactivation of wild-type and mutant bTIMs and tTIMs.** The inactivation constants are represented as a function of the temperature. The enzyme is considered inactive when its k_{inact} value reaches 0.001 s^{-1}. ●, H12N/K13G bTIM; ○, K13G bTIM; ■, H12N bTIM; □, bTIM; ▲, tTIM; △, H12N/K13G tTIM.

with the same half-life at 96 °C.

The thermostability observed for wild-type recombinant bTIM (half-life of 11.5 min at 68 °C) is in agreement with the growth temperature of the corresponding strain. H12N/K13G bTIM displayed poor thermostability, with an inactivation temperature of 37 °C. In the case of bTIM single mutants, H12N bTIM has a slightly lower inactivation temperature than wild-type bTIM, with a half-life of 11.5 min at 64 °C, while K13G bTIM has a similar half-life at 51 °C. The thermostability data are summarized in Table II.

Structural Stability—A feature common to all thermophilic proteins is their high intrinsic structural stability, allowing conservation of their functional state at high temperatures. To investigate the ability of the substituted Asn and Gly residues to destabilize the overall structure of bTIM and tTIM, we compared the thermal unfolding of the mutant and wild-type TIMs by microcalorimetry. Neither in bTIM nor in tTIM did simultaneous H12N, K13G replacement alter the stability of the enzyme. Half-denaturation temperatures (T_d) of 102 and 105 °C were recorded for wild-type tTIM and H12N/K13G tTIM, respectively. The double mutant is thus slightly more stable than the wild-type protein. For bTIM, the wild-type protein proved slightly more stable than the H12N/K13G double mutant, the difference in T_d being only 3 °C (76 *versus* 73 °C). The H12N bTIM single mutant appeared about as stable as the wild type (T_d of 77 °C), and K13G bTIM appeared slightly less stable (T_d of 73 °C, again 3 °C less than the T_d of wild-type bTIM). These data are summarized in Table II.

X-ray Structure of the H12N/K13G bTIM Mutant—The structure of the H12N/K13G bTIM mutant, complexed with the competitive inhibitor 2-phosphoglycolate, was refined to a model with good geometry and crystallographic quality (Table I). The x-ray structure consists of residues 1–250 for both subunits (Fig. 2). There was no clear density for the C-terminal His^{251} and Glu^{252} of either subunit. Some side chains or side-chain atoms exhibited no density in any electron density map and were not included in the structure. The stereochemical quality of the structure was analyzed with PROCHECK (50). All stereochemical parameters for the main-chain and side-chain atoms fall under the PROCHECK qualification "better."

Residue 230, defined as a proline in the sequence, is clearly an alanine, given the lack of available space for a proline residue and the clear electron density. In the native structure,

TABLE II
Summary of structural and enzymatic stabilities

The values of inactivation temperatures were derived at the inactivation point (k_{intact} = 0.001 s^{-1}) corresponding to a half-life of 11.5 min. $t½$ was calculated according to the following formula: $t½ = 0.69/k_{intact}$.

	Structural stability, T_d	Enzymatic stability, $t½$ = 11.5 min at T
	°C	
bTIM		
Wild type	76	68
H12N	77	64
H13G	73	51
H12N/K13G	73	37
tTIM		
Wild type	102	94
H12N/K13G	105	96

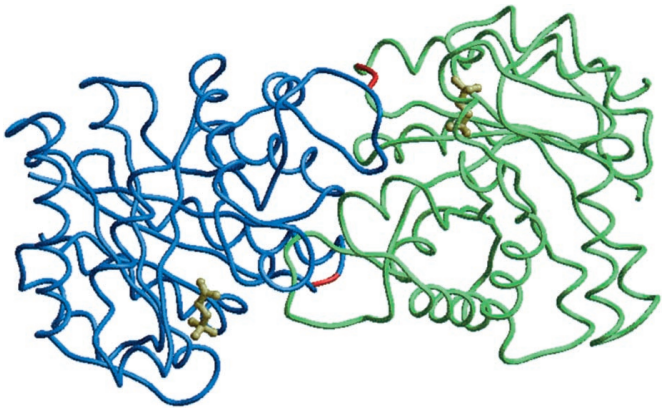

FIG. 2. **X-ray structure of H12N/K13G bTIM.** The Cα trace of each subunit is represented (*green*, subunit A; *blue*, subunit B). One molecule of 2-phosphoglycolate (*yellow*) occupies the active site of each subunit. The mutated region is represented in *red*.

this is probably also the case, because no Cγ and Cδ atoms were included for this residue in either subunit.

Both subunits are very similar, with an r.m.s. deviation of 0.24 Å for all main-chain atoms. Loops 5–7 are in the closed conformation in both subunits, due to the 2-phosphoglycolate ion occupying the active site of both subunits (Fig. 2). 121 water molecules were included in the structure with an average *B*-factor of 29.7 $Å^2$.

The structure of this mutant is very similar to that of native bTIM, with a Cα r.m.s. deviation of 0.27 Å for both subunits and an r.m.s. deviation of 0.33 and 0.39 Å, respectively, for all main-chain atoms and all atoms in both subunits (except the side-chain atoms of the mutated residues).

Fig. 3 shows the native and mutant bTIMs in the mutated region. One difference is a peptide flip of residue 12. As a consequence, a water molecule (*wat 2* in Fig. 3) is found in the mutant structure close to the position of the main-chain oxygen of His^{12} in the native structure. At the position of the side chain of Lys^{13} in the native structure, a structural water molecule (*wat 1* in Fig. 3) is found, making a long hydrogen bond to the main-chain oxygen of Leu^{237} (3.58 Å). The ND2 atom of Asn^{12} is located at the same position as the ND1 atom of His^{12} in the wild-type structure and makes the same contacts. Two structural waters (*wat 3* and *wat 4* in Fig. 3) are found hydrogen-bonded to this Asn^{12} ND2 atom. One of them (water 3) partially occupies the position of the NE2 atom of His^{12} in the wild-type structure; it makes contacts with main-chain atoms of Gly^{71} and Ala^{72} in the other subunit. Moreover, the OD1 atom of Asn^{12} also makes an intersubunit contact with the side chain of Gln^{70}. The second of these waters (water 4) is hydrogen-bonded to main-chain atoms of Asn^{8}, Trp^{9}, Gly^{233}, and Gly^{234}. The two

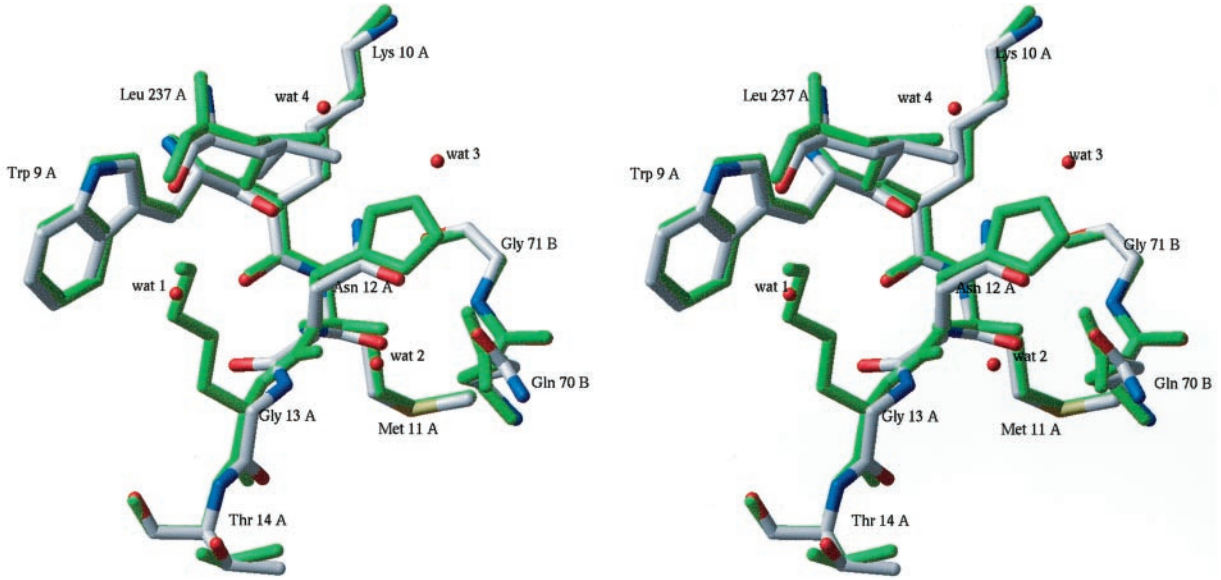

FIG. 3. **Stereo view of the loop 1 region of the bTIM (*green*) and H12N/K13G bTIM (*CPK color*) structures.** The residue names are given for H12N/K13G bTIM, and their respective subunits (A or B) are indicated. The four structural water molecules referred to under "Results" are represented (*wat 1* to *wat 4*), as well as Leu[237].

latter residues are located in the 3/10 helix of loop 8, stabilizing the phosphate of the ligand.

In the native structure, no waters were included because of its lower resolution. Hence, the last-mentioned water molecule (water 4) could be present in both structures. The other three water molecules are only present in the mutated structure, since there is not enough available space for a water molecule in the wild-type structure.

Molecular Dynamics Simulation—In order to better understand the influence of the mutations on the conformation of TIMs at high temperature, a molecular dynamics simulation of the flexibility of loop 1 was performed on bTIM and tTIM. A comparison of the geometries obtained after computational simulation clearly shows that the flexibility of loop 1 varies according to the structure (Fig. 4). According to the 20 dynamics simulation geometries represented in Fig. 4*E*, loop 1 appears considerably more rigid in tTIM than in bTIM, in agreement with our structural stability data.

To determine the roles of His[12] and Lys[13] in the adaptation of bTIM to high temperature, three additional structures were analyzed: H12N/K13G bTIM, H12N bTIM, and K13G bTIM. The substitution of an asparagine residue for His[12] does not significantly alter the flexibility of loop 1 (Fig. 4*C*), whereas substitution of a glycine residue for Lys[13] results in a large increase in the flexibility of loop 1 (Fig. 4, *B* and *D*). The greater flexibility appears to be due to the loss of a strong hydrogen bond between Lys[13] (NZ) and the main chain of Leu[237] occurring upon substitution of a glycine residue for Lys[13].

All molecular dynamics simulations are consistent with the enzyme stability and activity data.

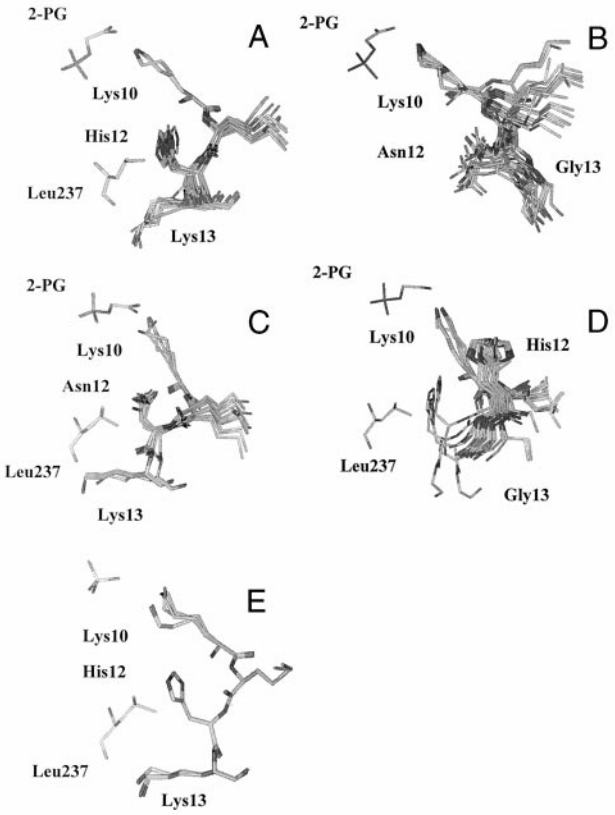

FIG. 4. **Molecular geometries of loop 1 generated by molecular dynamics simulation.** Residues 9–13 from loop 1 as well as Leu[237] and 2-phosphoglycolate (*2-PG*) are shown. 20 geometries obtained for bTIM (*A*), H12N/K13G bTIM (*B*), H12N bTIM (*C*), K13G bTIM (*D*), and tTIM (*E*) are represented.

DISCUSSION

Thermal inactivation of enzymes is often viewed as an alteration of protein structure with a concomitant decrease in enzyme activity. One type of change liable to alter the structure is deamidation of Asn/Gln residues. Studies on small peptides and proteins have shown that the rate of this reaction is considerably affected by temperature, pH, and ionic strength (30–32). At 37 °C and neutral pH, deamidation is very slow (it can take several days) (35), but it increases with increasing temperature. The residue Asn[12] located at the subunit interface is conserved in the TIMs of many mesophilic bacteria, but it is replaced by a histidine residue in thermophilic bTIM and tTIM. In both thermophilic TIMs studied here, not only is Asn[12] replaced by a histidine residue, but also Gly[13] is replaced by a lysine residue. In this context, it has been reported that an asparagine residue is considerably more sensitive to deamidation when followed by a glycine residue (34–36).

On the basis of the three-dimensional structure of bTIM, it

was previously proposed that replacement of Asn[12] by His could be an evolutionary adaptation of the enzyme to elevated temperatures; His[12] in bTIM would play a structural role similar to that of Asn[12] in mesophilic TIMs but would not be subject to deamidation at high temperature (17). This hypothesis is consistent with the observation that in yeast TIM, the Asn residues located at the interface of the enzyme (Asn[12] and Asn[77]) are very unstable at high temperature, leading to irreversible inactivation of the enzyme (52).

These considerations led us to examine the role of each residue separately and of the two combined to see how the replacement of Asn[12] by His and the presence of a Lys at position 13 might correlate with high thermal stability in thermophilic TIMs. To this end, we replaced both residues, individually and in combination, with those naturally present in most mesophilic TIMs. Replacement of both residues in bTIM causes a dramatic decrease in enzyme activity; the inactivation temperature of the double mutant is 37 °C ($t_{1/2}$ = 11.5 min). Since deamidation is usually very slow at this temperature, and since microcalorimetric studies show that the double mutation does not affect the overall structural integrity of bTIM, we believe that the observed inactivation is not related to deamidation. Confirmation of this assumption was obtained when the single His[12] to Asn substitution was performed. Indeed, H12N bTIM appears only slightly less stable than the wild-type enzyme (a 3 °C difference in T_d, $t_{½}$ = 11.5 min at 64 °C). Therefore, it can be concluded that deamidation is very slow at 64 °C and not responsible for inactivation of the bTIM double mutant at high temperature. Furthermore, we suggest that enzyme inactivation could be due to an alteration in the active site.

Wild-type and doubly mutated bTIM three-dimensional structures showed only slight differences, but this apparent similarity was not unexpected; at 20 °C, the temperature at which the crystals were grown, both enzymes display normal enzymatic activities. In the bTIM double mutant structure, the hydrogen bond between position 12 and the carbonyl oxygen of Trp[9] is conserved in the double mutant, because the Asn[12] side-chain amide nitrogen is located at the same place as the ND1 nitrogen of His[12] in wild-type bTIM. A unique difference between wild-type bTIM and doubly mutated bTIM was the loss of the hydrogen bond formed by the side chain of Lys[13] and the main chain of Leu[237]. We observe, however, that there is a structural water (*wat 1*) at the same position as Lys[13] NZ in the wild-type structure, forming a long hydrogen bond with Leu[237] (O) (Fig. 3). We believe that its presence could be necessary at moderate temperature to fill the cavity created by the K13G replacement. It should be mentioned that the assigned water molecule (water 1) found in the bTIM double mutant structure is facing Trp[9] (distance ~4 Å). Recently, experimental evidence has demonstrated that cations can interact with the indole ring of Trp residues located at a distance of about 4 Å (53). Since monovalent cations and water molecules have comparable electron densities, it is often difficult to distinguish them. Consequently, we do not rule out the possibility that water 1 could, in fact, be a cation.

Since the comparison of these three-dimensional structures cannot provide a final explanation of the loss of enzymatic stability of the double mutant, we attempted to assess enzyme behavior at high temperature by molecular dynamics simulation. On the basis of these studies, we can propose a hypothesis to explain the marked decrease in enzyme activity observed in the bTIM double mutant. To date, the role of Lys[13] in thermophilic TIMs remains unclear. The structures of several mesophilic TIMs suggest that a Gly residue at this position does not interact significantly with its neighbors. On the contrary, the Lys[13] (NZ)–Leu[237] (O) hydrogen bond (2.68 Å) of wild-type bTIM stabilizes loop 1 and thereby favors the correct orientation of the Lys[10] side chain. This latter residue is part of the catalytic triad, and its correct orientation is crucial to the enzyme's activity, since the residue is involved in neutralizing the negatively charged intermediate during catalysis (54, 55). All TIM three-dimensional structures resolved to date show unusual ψ and ϕ angles for Lys[10]. In wild-type bTIM and H12N/K13G bTIM, the particular conformation of Lys[10] is maintained by several interactions, which are very similar in both structures (Table III). In the bTIM double mutant, because of the Gly residue at position 13, the Lys[13] (NZ)–Leu[237] (O) hydrogen bond cannot be formed. Molecular dynamics simulations on doubly mutated bTIM and K13G bTIM revealed a greater flexibility of loop 1 (Fig. 4, *B* and *D*). Consequently, we propose that the K13G replacement increases the flexibility of loop 1 and that at high energy levels (elevated temperatures), this greater flexibility could be responsible for a major deviation of the Lys[10] side chain, resulting in decreased enzyme activity without any alteration of the enzyme's structural stability. This assumption is in agreement with our enzymatic stability assays, clearly showing that the presence of glycine in H12N/K13G bTIM and K13G bTIM results in rapid inactivation at 37 and 51 °C, respectively. The water molecule (or cation) observed at this position in the crystal structure is unable to rigidify loop 1. It is worth stressing that we performed the theoretical simulations on the single mutants (H12N and K13G mutants of bTIM) before the experimental test. They foretold a dramatic effect of K13G and a lesser effect of H12N on bTIM stability. The theoretical simulation thus proved a useful and reliable predictive tool in this study.

TABLE III
Hydrogen bonds stabilizing Lys[10] residue (subunit A)

Contacts	Wild-type bTIM	H12N/K13G bTIM
	Å	
Lys[10] (O) → Trp[9] (O)	2.95	3.02
Lys[10] (O) → Met[11] (N)	2.24	2.24
Lys[10] (O) → His/Asn[12] (N)	3.01	3.03
Lys[10] (O) → Gln[63] (OE1)	3.31	3.22
Lys[10] (O) → Gln[63] (NE2)	2.86	2.80
Lys[10] (N) → Asn[8] (O)	3.23	3.12
Lys[10] (N) → Asn[8] (OD1)	3.13	3.11
Lys[10] (N) → Trp[9] (O)	2.26	2.26
Lys[10] (N) → Trp[9] (N)	2.72	2.70
Lys[10] (N) → Met[11] (N)	3.57	3.56
Lys[10] (N) → Gln[63] (OE1)	3.35	3.65
Lys[10] (N) → Gln[63] (NE2)	2.89	2.88
His[12] (ND1) → Trp[9] (O)	3.01	
Asn[12] (ND2) → Trp[9] (O)		2.77
Lys[13] (NZ) → Leu[237] (O)	2.68	

The double mutation was also created in tTIM. We show that it does not diminish the activity of the enzyme, in contrast to its effect in the bTIM double mutant; the respective inactivation temperatures of the wild-type and doubly mutated tTIM are 94 and 96 °C. In our microcalorimetric experiments, moreover, the double mutant and wild-type tTIM display a similar resistance to high temperature (T_d values of 105 and 102 °C, respectively), thus confirming their high structural and enzymatic stability (Table III). These results are in agreement with those of Beaucamp *et al*. (24). On the basis of the available results, one can speculate that the high enzymatic stability of the tTIM double mutant could be due to many interactions compensating for the loop 1 instability introduced by the K13G mutation. The molecular dynamic simulations performed on the wild-type tTIM structure are consistent with this hypothesis. At energy levels corresponding to high temperatures, the tTIM loop 1 displays very restricted molecular movement, probably resulting from the high stability of the whole structure. This high stability is also ob-

served in the region corresponding to loop 1, which thus appears quite insensitive to the K13G mutation. The extreme thermostability of tTIM has recently been correlated with a high number of salt bridges and a large network of interactions resulting from dimer-dimer assembly of the protein in solution.[2]

His[12] and/or Lys[13] residues have also been found in the TIMs of certain mesophilic strains (25, 27, 28),[3] but none of these TIMs have yet been characterized, notably as regards to their thermostability. Some enzymes of mesophilic strains can display moderately thermophilic features, as is the case of subtilisin (56), pyrophosphate phosphohydrolase (57), and the Trp RNA-binding attenuation protein (58) of *B. subtilis.* Consequently, we cannot draw any general conclusions as to the relationship between the presence of these residues and TIM thermostability.

We nevertheless show that Lys[13] in bTIM plays a crucial role in the enzyme's functional adaptation to high temperature and that the presence of this residue in other TIMs is not detrimental to their activity at medium range temperatures. In a recent report on *Thermus thermophilus* 3-isopropylmalate dehydrogenase, the authors strongly suggest a very close relationship between conformational flexibility and enzyme function (59). Our work is in agreement with this line of thought, and we further show that a noncatalytic residue (Lys[13]) is essential to the activity of bTIM at high temperature.

In the present work, we propose a new approach to the entangled problem of molecular adaptation to extreme temperatures: a combination of site-directed mutagenesis, differential scanning calorimetry, x-ray crystallography, and molecular dynamics simulation.

Our results are consistent with the conclusion that no general rules can be drawn concerning the molecular adaptation of proteins to high temperature, each protein "designing" its own molecular mechanism for adapting to extreme conditions (60).

It has been established that the difference in free energy of stabilization ($\Delta\Delta G_{N \rightarrow U}$) between mesophilic and (hyper)thermophilic enzymes is equivalent to about 100 kJ/mol (26, 61). This led to the conclusion that the energy required to stabilize the overall structure of a thermophilic protein could be brought in by a few additional hydrogen bonds, ion pairs, or hydrophobic interactions (1). Our results demonstrate that adaptation of an enzyme to high temperature cannot be reduced to the sole stabilization of its overall structure, but that it also, and perhaps more importantly, implies stabilization of the active site.

Acknowledgments—We thank N. Glansdorff for providing the *T. maritima* genomic DNA and Dr. J. M. François for stimulating discussions.

REFERENCES

1. Jaenicke, R., Schurig, H., Beaucamp, N., and Ostendorp, R. (1996) *Adv. Protein Chem.* **48,** 181–269
2. Russel, R. J., and Tylor, G. L. (1995) *Curr. Opin. Biotechnol.* **6,** 370–374
3. Rice, D. W., Yip, K. S., Stillman, T. J., Britton, K. L., Fuentes, A., Connerton, I., Pasquo, A., Scandura, R., and Engel, P. C. (1996) *FEMS Microbiol. Rev.* **18,** 105–117
4. Pfeil, W., Gesierich, U., Kleeman, G. R., and Sterner, R. (1997) *J. Mol. Biol.* **272,** 591–596
5. Peters, J., Baumeister, W., and Lupas, A. (1996) *J. Mol. Biol.* **257,** 1031–1041
6. Hennig, M., Sterner, R., Kirschner, K., and Jansonius, J. N. (1997) *Biochemistry* **36,** 6009–6016
7. Lim, J. H., Yu, Y. G., Han, Y. S., Cho, S., Ahn, B. Y., Kim, S. H., and Cho, Y. (1997) *J. Mol. Biol.* **270,** 259–274
8. Huber, R., Langworthy, T. A., König, H., Thomm, M., Woese, C. R., Sleytr, U. B., and Stetter, K. O. (1986) *Arch. Microbiol.* **144,** 324–333
9. Fahey, R. C., Kalb, E., and Harris, J. I. (1971) *Biochem. J.* **124,** 77P
10. Rieder, S. V., and Rose, I. A. (1959) *J. Biol. Chem.* **234,** 1007–1010
11. Farber, G. K., and Petsko, G. A. (1990) *Trends Biochem. Sci.* **15,** 228–234
12. Banner, D. W., Bloomer, A. C., Petsko, G. A., Philips, D. C., Pogson, C. I., Wilson, I. A., Corran, P. H., Furth, A. J., Milman, J. D., Offord, R. E., Priddle, J. D., and Waley, S. G. (1975) *Nature* **255,** 609–614
13. Lolis, E., Alber, T., Davenport, R. C., Rose, D., Hartman, F. C., and Petsko, G. A. (1990) *Biochemistry* **29,** 6609–6618
14. Wierenga, R. K., Noble, M. E. M., Vriend, G., Nauche, S., and Hol, W. G. J. (1991) *J. Mol. Biol.* **220,** 995–1015
15. Noble, M. E. M., Zeelen, J. P., Wierenga, R. K., Mainfroid, V., Goraj, K., Gohimont, A.-C., and Martial, J. A. (1993) *Acta Crystallogr. Sec. D* **49,** 403–417
16. Mande, S. C., Mainfroid, V., Kalk, K. H., Goraj, K., Martial, J. A., and Hol, W. G. J. (1994) *Protein Sci.* **3,** 810–821
17. Delboni, L. F., Mande, S. C., Rentier-Delrue, F., Mainfroid, V., Turley, S., Vellieux, M. D., Martial, J. A., and Hol, W. G. J. (1995) *Protein Sci.* **4,** 2594–2604
18. Velanker, S. S., Ray, S. S., Gokhale, R. S., Hemalatha Balaram, S. S., and Murthy, M. R. N. (1997) *Structure* **5,** 751–761
19. Alvarez, M., Zeelen, J. P., Mainfroid, V., Rentier-Delrue, F., Martial, J. A., Wyns, L., Wierenga, R. K., and Maes, D. (1998) *J. Biol. Chem.* **273,** 2199–2206
20. Maldonado, E., Soriano-Garcia, M., Moreno, A., Cabrera, N., Garza-Ramos, G., Tuena, de Gomez-Puyou, M., Gomez-Puyou, A., Perez-Monfort, R. (1998) *J. Mol. Biol.* **283,** 193–203
21. Williams, J. C., Zeelen, J. Ph., Neubauer, G., Vriend, G., Backmann, J., Michels, P. A. M., Lambeir, A.-M., and Wierenga, R. K. (1999) *Protein Eng.* **12,** 243–250
22. Rentier-Delrue, F., Mande, S. C., Moyens, S., Terpstra, P., Mainfroid, V., Goraj, K., Hol, W. G. J., and Martial, J. A. (1993) *J. Mol. Biol.* **229,** 85–93
23. Schurig, H., Beaucamp, N., Ostendorp, R., Jaenicke, R., Adler, E., and Knowles, J. R. (1995) *EMBO J.* **14,** 442–451
24. Beaucamp, N., Hofmann, A., Kellerer, B., and Jaenicke, R. (1997) *Protein Sci.* **6,** 2159–2165
25. Kaneko, T., Tanaka, A., Sato, S., Kotani, H., Sazuka, T., Miyajima, N., Sugiura, M., and Tabata, S. (1995) *DNA Res.* **2,** 153–166
26. Pfeil, W. (1998) *Protein Stability and Folding: A Collection of Thermodynamics Data*, Springer, Berlin, Heidelberg
27. Gebbia, J. A., Backenson, P. B., Coleman, J. L., Anda, P., and Benach, J. L. (1997) *Gene* (*Amst.*) **188,** 221–228
28. Leyva-Vazquez, M. A., and Setlow, P. (1994) *J. Bacteriol.* **176,** 3903–3910
29. Yuan, P. M., Talent, J. M., and Gracy, R. W. (1981) *Mech. Ageing Dev.* **17,** 151–162
30. Tyler-Cross, R., and Schirch, V. (1991) *J. Biol. Chem.* **266,** 22549–22556
31. Tomazic, S. J., and Klibanov, A. M. (1988) *J. Biol. Chem.* **263,** 3086–3091
32. Hayes, C. S., and Setlow, P., (1997) *J. Bacteriol.* **179,** 6020–6027
33. Chen, H., Ford, C., and Reilly, P. J. (1994) *Biochem. J.* **301,** 275–281
34. Kossiakoff, A. A. (1988) *Science* **240,** 191–194
35. Stephenson, R. C., and Clarke, S. (1989) *J. Biol. Chem.* **264,** 6164–6170
36. Wright, H. T. (1991) *Protein Eng.* **4,** 283–294
37. Tomizawa, H., Yamada, H., Hashimoto, Y., and Imoto, T. (1995) *Protein Eng.* **8,** 1023–1028
38. Gracy, R. W., Lu, H. S., Yuan, P. M., and Talent, J. M. (1983) in *Altered Proteins and Ageing* (Adelman, R. C., and Roth, G. S., eds) pp 27–34, CRC Press, Inc., Boca Raton, FL
39. Casal, J. I., Ahern, T. J., Davenport, R. C., Petsko, G. A., and Klibanov, A. M. (1987) *Biochemistry* **26,** 1258–1264
40. L'Hoir, C., Renard, A., and Martial, J. A. (1990) *Gene* (*Amst.*) **89,** 47–52
41. Rosenberg, A. H., Lade, B. N., Chui, D. S., Lin, S. W., Dunn, J. J., and Studier, F. W. (1987) *Gene* (*Amst.*) **56,** 125–135
42. Ochman, H., Medhora, M. M., Garza, D., and Hartl, D. L. (1990) in *PCR Protocols: A Guide to Methods and Applications* (Innis, M. A., Gelfand, D. H., Sninsky, J. J., and White, T. J.) pp. 219–227, Academic Press, Inc., San Diego
43. Studier, F. W., and Moffatt, B. A. (1986) *J. Mol. Biol.* **189,** 113–130
44. Misset, O., and Opperdoes, F. (1984) *Eur. J. Biochem.* **144,** 475–483
45. Otwinowski, Z. (1993) *DENZO: An Oscillation Data Processing Program for Macromolecule Crystallography*, Yale University, New Haven, CT
46. Collaborative Computational Project 4 (1994) *Acta Crystallogr. Sec. D* **50,** 760–763
47. Jones, T. A., Zou, J. Y., Cowan, S. W., and Kjelgaard, M. (1991) *Acta Crystallogr. Sec. A* **47,** 110–119
48. Brünger, A. T. (1992) *X-PLOR: A System for X-ray Crystallography and NMR*, Version 3.1, Yale University Press, New Haven, CT
49. Brünger, A. T., Adams, P. D., Clore, M. G., DeLano, W. L., Gros, P., Grosse-Kunstleve, R. W., Jiang, J. S., Kuszewski, J., Nilges, M., Pannu, N. S., Read, R. J., Rice, L. M., Simonson, T., and Warren, G. L. (1998) *Acta Crystallogr. Sec. D* **54,** 905–921
50. Laskowski, R. A., MacArthur, M. W., Moss, D. S., and Thornton, J. M. (1993) *J. Appl. Crystallogr.* **24,** 946–950
51. Vriend, G. (1990) *J. Mol. Graphics* **8,** 52–56
52. Ahern, T. J., Casal, J. I., Petsko, G. A., and Klibanov, A. M. (1987) *Proc. Natl. Acad. Sci. U. S. A.* **84,** 675–679
53. Wouters, J. (1998) *Protein Sci.* **7,** 2472–2475
54. McCarthy, D. J., Lolis, E., Komives, E. A., and Petsko, G. A. (1994) *Biochemistry* **33,** 2815–2823
55. Lodi, P. J., Chang, L. C., Knowles, J. R., and Komives, E. A. (1994) *Biochemistry* **33,** 2809–2814
56. Kamal, M., Hoog, J. O., Kaiser, R., Shafqat, J., Razzaki, T., Zaidi, Z. H., and Jornvall, H. (1995) *FEBS Lett.* **374,** 363–366
57. Shimizu, T., Imai, M., Araki., S., Kishida, K., Terasawa, Y., and Hachimori, A. (1997) *Int. J. Biochem. Cell Biol.* **29,** 303–310
58. Baumann, C., Xirasagar, S., and Gollnick, P. (1997) *J. Biol. Chem.* **272,** 19863–19869
59. Zavodszky, P., Kardos, J., Svingor, A., and Petsko, G. A. (1998) *Proc. Natl. Acad. Sci. U. S. A.* **95,** 7406–7411
60. Jaenicke, R. (1991) *Eur. J. Biochem.* **202,** 715–728
61. Grättinger, M., Dankesreiter, A., Schurig, H., Jaenicke, R. (1998) *J. Mol. Biol.* **280,** 525–533